Have gravitomagnetic induction fields already been observed in the laboratory?

Jacob Biemond*

Vrije Universiteit, Amsterdam, Section: Nuclear magnetic resonance, 1971-1975
**Postal address: Sansovinostraat 28, 5624 JX Eindhoven, The Netherlands*
Website: http://www.gravito.nl Email: j.biemond@gravito.nl

ABSTRACT

In 1980 Woodward reported generation of induced electric charges Q in falling cylinders of copper, steel and aluminium. In 1982 he also reported induced electric charges in rotating cylinders of different metals. In order to explain these observations, Woodward used a generalization of Maxwell's equations, proposed by Luchak. These equations contain the gravitational field, but their predictions appeared to be not quite satisfactory. Since that time, no attempts have been made to explain the observed charges. Previously, related experiments on rotating metal cylinders were carried out by Surdin in 1977 and 1980. He reported reversing magnetic induction fields near rotating cylinders of bronze and tungsten.

In this work a renewed analysis of the observations above is given, applying a special interpretation of the gravitomagnetic equations, deduced from general relativity. In this approach it is assumed that the gravitomagnetic field is equivalent to the magnetic induction field from electromagnetic origin. Formulas for the generated gravitomagnetic field, the induced voltage and induced charge Q in Woodward's falling cylinders have been deduced. The predicted charges are proportional to the impact velocity, but are an order of magnitude smaller than the observed charges. The magnetic induction fields observed by Surdin are in agreement with the predictions from the proposed theory, but no explanation for the reversal of these fields has been given.

1. INTRODUCTION

Exploring a possible coupling between electromagnetic and gravitational fields, Woodward [1] reported induced electric charges in cylinders of different metals, falling onto an impact plate. Moreover, he discussed a number of tests that seemed to rule out conventional charge generation mechanisms as the source of the observed signals. In addition, Woodward also detected induced charges in rotating cylinders of brass and aluminium [2]. Previously, related experiments on rotating cylinders of bronze and tungsten were carried out by Surdin [3, 4]. He detected reversing magnetic induction fields around these cylinders.

In order to explain the observed charges, Woodward [1] used a unified five-dimensional theory, proposed by Luchak [5], connecting the electromagnetic field to the gravitational field. In line with this theoretical approach, he tested the relation

$$Q = \beta^* m\, g = \beta^* m \frac{\Delta v_z}{\Delta t}, \tag{1.1}$$

where Q is the induced charge, m is the mass of the cylinder and g is the gravitational acceleration. The latter quantity was approximated by $\Delta v_z/\Delta t$, where $\Delta v_z = v_z$ is the impact velocity of the falling cylinder hitting the impact plate and Δt is the time in which the speed v_z reduces from value v_z to zero. Woodward adopted a constant value of Δt for all measurements. The observed charges Q appeared to be nearly independent on the mass m of the cylinders and appeared to be approximately proportional to the impact velocity Δv_z. So, the parameter β^* is approximately constant for a chosen metal, but varied somewhat

for copper, steel and aluminium. Woodward concluded that his observations may be explained by coupling between the electromagnetic and the gravitational field.

In this work it is tried to explain the observed induced charges of ref. [1] by a special interpretation of the gravitomagnetic theory, which may be deduced from general relativity [6–8]. In this approach the so-called "magnetic-type" gravitational field is identified as a common magnetic induction field. Several alternative formulations of the gravitomagnetic equations deduced from general relativity have been given by many authors (see for a discussion refs. [6–8] and references therein).

In section 2 of this paper we will first calculate the φ-component B_φ of the gravitomagnetic field generated in the falling cylinder. Using the induction equation from electromagnetism, the corresponding induced charge is calculated in section 3. Subsequently, the predicted charges are compared with those observed by Woodward [1]. In section 4 the related gravitomagnetic field of a rotating cylinder is calculated. The predicted values of this field are compared with observed magnetic induction fields observed by Surdin [3, 4]. A final discussion of the results is given in section 5.

2. CALCULATION OF THE GRAVITOMAGNETIC FIELD $\mathbf{B}_\varphi$

In our approach the following set of four differential equations for sources in vacuum, expressed in SI units, may be deduced from general relativity [6–8]

$$\nabla \times \mathbf{B} = -\frac{\beta \mu_0 G^{1/2}}{k^{1/2}} \rho \mathbf{v} + \frac{\beta \mu_0}{4\pi k^{1/2} G^{1/2}} \frac{\partial \mathbf{g}}{\partial t}, \tag{2.1}$$

$$\nabla \cdot \mathbf{g} = -4\pi G \rho, \tag{2.2}$$

$$\nabla \times \mathbf{g} = -\frac{G^{1/2}}{\beta k^{1/2}} \frac{\partial \mathbf{B}}{\partial t}, \tag{2.3}$$

$$\nabla \cdot \mathbf{B} = 0, \tag{2.4}$$

where $\mathbf{B} = \mathbf{B}$(gm) is the gravitomagnetic field (note that this field has the same dimension as the magnetic induction field $\mathbf{B}$(em) in electromagnetism). The constant μ_0 is the vacuum permeability, ρ is the mass density and $\mathbf{g}$ is the gravitational field. The parameter $k = (4\pi\varepsilon_0)^{-1} = 8.9876\times10^9$ N.m^2.C^{-2} is the constant in Coulomb's law, analogously written to the gravitational constant G in Newton's gravitation law. Compare

$$\mathbf{F}_{\text{Coulomb}} = k \frac{Q_1 Q_2}{R^3} \mathbf{R} \quad \text{and} \quad \mathbf{F}_{\text{Newton}} = -G \frac{m_1 m_2}{R^3} \mathbf{R}. \tag{2.5}$$

Note that for the choice of the dimensionless quantity $\beta = +1$, the analogy between the gravitomagnetic equations (2.1)–(2.4) and the Maxwell equations is striking. The sign and the value of β, however, does not follow from the deduction. Many different values for β are chosen in the literature (see discussions in refs. [7, 8]).

It is noticed that only rotational velocities may be allowed in eq. (2.1), implying that $\mathbf{v} = \boldsymbol{\omega} \times \mathbf{r}$ ($\boldsymbol{\omega}$ is the angular velocity of a mass element $\rho\, dV$ and $\mathbf{r}$ is the distance from the rotation axis to this mass element). Translational motion has been excluded by several authors, for example by Blackett [9]. This exclusion may be based on the outcome of an experiment of a swinging bar in a laboratory, performed by Wilson [10]. However, in order to check the magnitude of a possible translational contribution to the field $\mathbf{B}$(gm) in (2.1), we first include translational motion. Application of Stokes' theorem to (2.1) then yields

$$\iint (\nabla \times \mathbf{B}) \cdot \mathrm{d}\mathbf{S} = \oint \mathbf{B} \cdot \mathrm{d}\mathbf{s} = -\frac{\beta \mu_0 G^{1/2}}{k^{1/2}} \iint \rho \mathbf{v} \cdot \mathrm{d}\mathbf{S} + \frac{\beta \mu_0}{4\pi k^{1/2} G^{1/2}} \iint \frac{\partial \mathbf{g}}{\partial t} \cdot \mathrm{d}\mathbf{S}. \qquad (2.6)$$

When a metal cylinder of radius r_0 and height h is falling vertically from an height $z_1 = 0$, the speed at height z and time t will be denoted by $\mathbf{v}_z$. The cylinder is translationally accelerated in Earth's gravitational field $\mathbf{g} = -(GM/R^2)\mathbf{R}/R = g\mathbf{R}/R$ (see figure 1). Calculation from (2.6) then yields for the total φ-component B_φ of the field $\mathbf{B}$ inside the cylinder of radius r

$$B_\varphi = B_{\varphi 1} + B_{\varphi 2} = -\frac{\beta \mu_0 G^{1/2}}{2\pi k^{1/2}} \frac{m v_z}{r h} - \frac{\beta \mu_0 g r v_z}{4\pi k^{1/2} G^{1/2} R}, \qquad (2.7)$$

where m is the mass of the cylinder. Earth's radius R is given by $R_\oplus = 6.371\times10^6$ m and the gravitational acceleration g by $g = -GM/R^2 = -9.82$ m.s^{-2} (Earth's mass is $M = M_\oplus = 5.973\times10^{24}$ kg). It is noticed that the contribution $B_{\varphi 1}$ is proportional to m and v_z, and displays a singularity at $r \to 0$. The contribution $B_{\varphi 2}$ is proportional to g, v_z and r. Only the contribution $\mathbf{B}_\varphi = \mathbf{B}_{\varphi 2}$ is shown in figure 1. For an inclination angle of θ between the direction of $\mathbf{g}$ and $\mathbf{v}$, a factor $\cos\theta$ has to be added to both terms on the right hand side of (2.7) (compare with discussion of Woodward [1] on this issue).

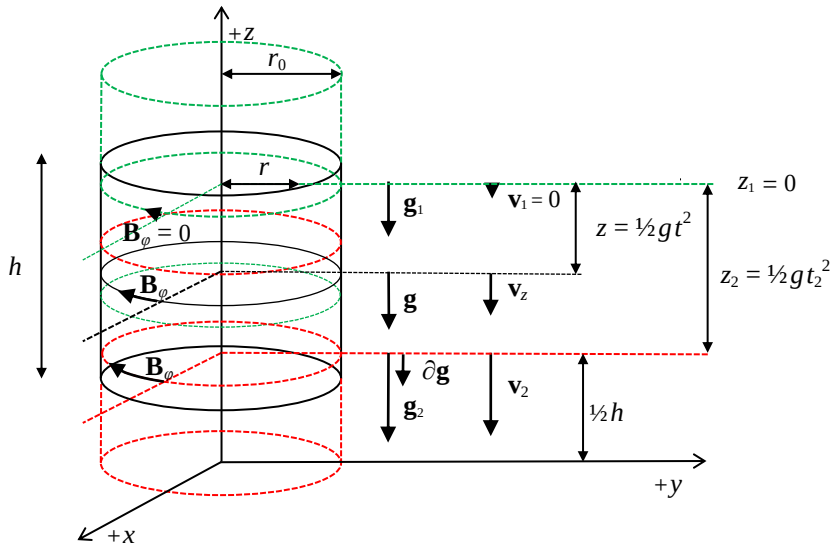

Figure 1. The centre of a metal cylinder of radius r_0 and height h is initially located at height $z_1 = 0$. At the plane through the centre and perpendicular to the axis of the cylinder, the gravitational field is given by $\mathbf{g}_1$. The initial speed $\mathbf{v}_1$ and gravitomagnetic field $\mathbf{B}_\varphi = \mathbf{B}_{\varphi 2}$ are then zero. At height z, the gravitational field strength is $\mathbf{g}$, the speed is $v_z = gt$ and z is given by $z = \frac{1}{2}gt^2$, whereas the φ-component $B_\varphi = B_{\varphi 2}$ of the gravitomagnetic field is given by (2.7b). Just before hitting the impact plate at time t_2, the gravitational field is $\mathbf{g}_2$ ($\partial\mathbf{g} = \mathbf{g}_2 - \mathbf{g}_1$). The field $\mathbf{B}_{\varphi 2}$, as well as the speed $v_2 = gt_2$ are then at a maximum, whereas $z_2 = \frac{1}{2}gt_2^2$.

As an illustration of the magnitude of the quantities occurring in (2.7), one may use an experiment carried out by Woodward [1]. We consider his copper cylinder with mass $m = 1.233$ kg, radius $r_0 = 0.025$ m, height $h = 0.08$ m and impact speed of $v_z = v_2 = gt_2 = -1.00$ m.s^{-1}, implying $t_2 = 0.102$ s and $z_2 = -0.0509$ m. Calculation of the fields $B_{\varphi 1}$ and $B_{\varphi 2}$ from (2.7) yields, respectively

$$B_{\varphi 1} = +1.06\times10^{-14}\beta \text{ T}, \quad B_{\varphi 2} = -4.98\times10^{-15}\beta \text{ T}. \qquad (2.8)$$

So, for this example the contribution $|B_{\varphi 1}|$ is about twice as large as $|B_{\varphi 2}|$. At present, direct measurement of these contributions to B_φ seems to be impossible, but below it is discussed how consequences of these fields may become manifest.

3 CALCULATION OF THE CHARGES

When the field B_φ of (2.7) is generated in a falling cylinder, it will disappear by some mechanism. For a perfectly elastic collision of the cylinder the weak field B_φ of (2.7) would reduce to zero value by returning to its initial position $z_1 = 0$, but the collision is probably nearly completely inelastic. Since the applied guiding mechanism prevents rotation of the cylinders in Woodward's experiments, the field B_φ may also not vanish by action of eq. (2.3). However, when the gravitomagnetic field is equivalent to the magnetic induction field in electromagnetism, generation of an electric field **E**, according to the Faraday-Maxwell equation, may be the easiest way to eliminate the field B_φ of (2.7)

$$\nabla \times \mathbf{E} = -\frac{\partial \mathbf{B}}{\partial t}. \tag{3.1}$$

Application of Stokes' theorem to a surface **S** (see figure 2) yields

$$\oiint (\nabla \times \mathbf{E}) \cdot \mathrm{d}\mathbf{S} = \oint \mathbf{E} \cdot \mathrm{d}\mathbf{s} = V_{ind} = -\oiint \frac{\partial \mathbf{B}}{\partial t} \cdot \mathrm{d}\mathbf{S} = +\int_0^{r_0} \frac{\partial B_\varphi}{\partial t} h\, dr, \tag{3.2}$$

where V_{ind} is the induced voltage and $\partial \mathbf{B} = -\mathbf{B}_\varphi$. It will be assumed in figure 2 that only the component $B_{\varphi 2}$ of B_φ in (2.7) differs from zero value.

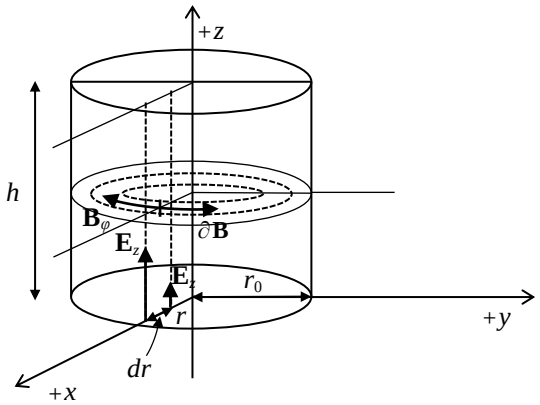

Figure 2. The location of the cylinder just before hitting the impact plate is drawn, where speed $v_z = gt$ and height $z = \frac{1}{2}gt^2$. The vanishing gravitomagnetic field $\mathbf{B}_\varphi = \mathbf{B}_{\varphi 2}$ perpendicular to, e.g., the *x*-*z* plane may induce an electric field $\mathbf{E}_z$ in the plane through the *z*-axis of the cylinder and the *x*-axis. The total surface of the rectangle with sides *h* and r_0 is given by $S = hr_0$ with $dS = h dr$, whereas **n** is the unit vector perpendicular to the *x*-*z* plane (so $\mathbf{B}_\varphi = -B_\varphi \mathbf{n}$ and $\mathbf{S} = S\mathbf{n}$). The coordinate *r* is lying in the interval $0 \le r \le r_0$.

In view of Woodward's figure 3 for a cylinder of copper falling onto an impact plate described in ref. [1], we will assume generation of a damped harmonic magnetic induction field of the form

$$\frac{\partial B_{\varphi 2}}{\partial t} = \frac{-\partial\left\{\left(\cos\omega_1 t + \cos\omega t\right) e^{-at} B_{\varphi 2}(r)\right\}}{\partial t} = \frac{-\partial\left\{\left(\cos\omega_1 t + \cos\omega t\right) e^{-at}\right\}}{\partial t} B_{\varphi 2}(r), \tag{3.3}$$

where $B_{\varphi 2}(r)$ is given in (2.7) (the speed v_z of the cylinder is constant from top to bottom). The quantity a is a constant and ω_1 and ω are the angular frequencies of the harmonic oscillations of $B_{\varphi 2}(r)$. Insertion of (3.3) into (3.2), followed by integration from $r = 0$ to $r = r_0$ yields

$$V_{ind} = -\frac{\partial\left\{\left(\cos\omega_1 t + \cos\omega t\right)e^{-at}\right\}}{\partial t} h \int_0^{r_0} B_{\varphi 2}(r)\,dr = -\tfrac{1}{2}\, f(t)\, h\, r_0 B_{\varphi 2}(r_0), \qquad (3.4)$$

where $f(t)$ is defined by

$$f(t) \equiv -\left\{\omega_1 \sin\omega_1 t + \omega \sin\omega t + a\left(\cos\omega_1 t + \cos\omega t\right)\right\} e^{-at} = \left(g1 + g2 + g3\right)e^{-at}. \qquad (3.5)$$

The functions *g1*, *g2* and *g3* are given by $-\omega_1 \sin\omega_1 t$, $-\omega \sin\omega t$ and $-a(\cos\omega_1 t + \cos\omega t)$, respectively.

Furthermore, one might add the contribution $B_{\varphi 1}(r)$ from (2.7) into (3.3). Integration analogous to (3.4), then leads to an additional contribution containing a factor $\ln r_0/r_1$, where r_1 approaches zero value. So, this contribution yields a singularity at $r_1 = 0$ in the induced voltage V_{ind}.

The following estimates may be extracted from Woodward's figure 3 [1]: $a = 1/(10^{-4})$ s^{-1}, $\omega_1 = 2\pi/(1.1\times10^{-4})$ s^{-1} and $\omega = 2\pi/(5.5\times10^{-4})$ s^{-1}. When these values are introduced into $f(t)$ of (3.5), the induced voltage V_{ind} of (3.4) can be calculated. Note that V_{ind} and $f(t)$ have the same sign. Calculation shows that $f(t)$ and also the quantity V_{ind} (compare (3.4) and (3.5)) become zero for the following values of t, for example: $t = -0.058\times10^{-4}$ s, $t = +0.565\times10^{-4}$ s, $t = 1.026\times10^{-4}$ s, $t = 2.692\times10^{-4}$ s and $t = 5.442\times10^{-4}$ s.

In our figure 3 the time dependence of function $f(t)$ and thus V_{ind} are shown as a function of t. In addition, the time dependences of the contributing functions *g1*, *g2* and *g3*

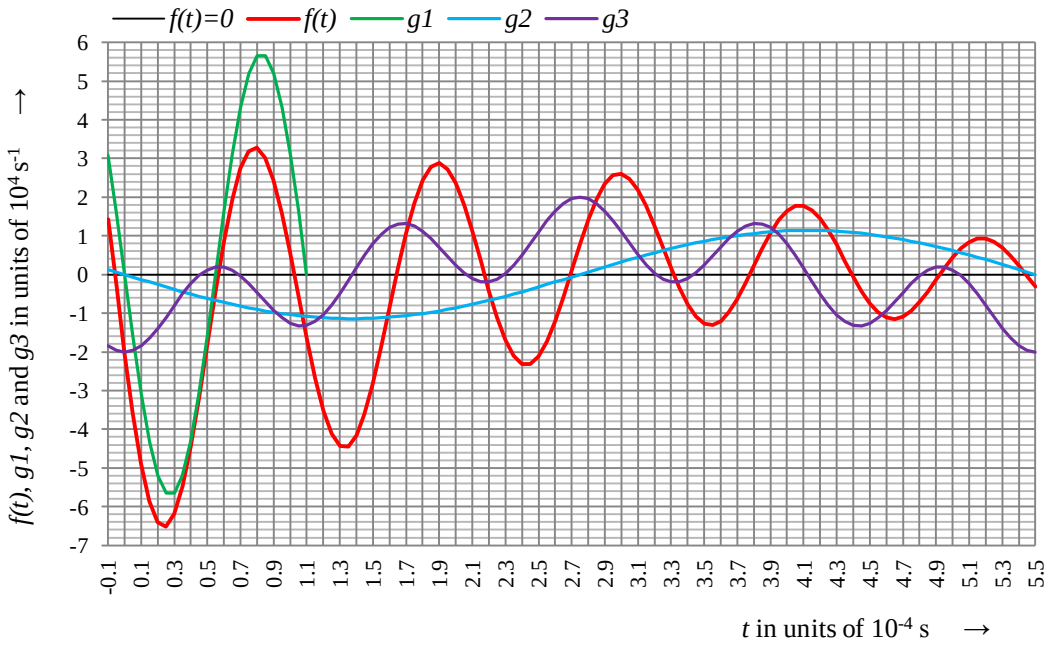

Figure 3. The function $f(t)$ (red curve) of (3.5) versus time t has been given for the time interval -0.1×10^{-4} s $< t < +5.5\times10^{-4}$ s. In addition, the function *g1* (green curve) has been shown for the time interval -0.1×10^{-4} s $< t < 1.1\times10^{-4}$ s, whereas the functions *g2* (blue curve) and *g3* (violet curve) have been given for the interval -0.1×10^{-4} s $< t < 5.5\times10^{-4}$ s. Term *g1* is the dominating term. Note that the time interval -0.058×10^{-4} s $< t < +5.442\times10^{-4}$ s has a length of 5.5×10^{-4} s.

are shown. For clarity reasons only one full cycle is given for the term *g1*. The functions *f*(*t*), *g1*, *g2* and *g3* are all expressed in units of 10^4 s^{-1}. It is noticed, that the shape of the red curve of the sum function *f*(*t*) is in qualitative agreement with the shape of Woodward's signal displayed in his figure 3. The agreement is better for the interval -0.058×10^{-4} s < *t* < $+1.026\times10^{-4}$ s than for the interval 2.692×10^{-4} s < *t* < 5.442×10^{-4} s. The width of the first subpulse of the curve *f*(*t*) can be calculated to be $\Delta t = 0.623\times10^{-4}$ s, compared to $\Delta t = 0.55\times10^{-4}$ s for the green curve of *g1*. Note that Woodward [1] used a width $\Delta t = 0.75\times10^{-4}$ s for the first subpulse *B* for all samples. He denoted the initial pulse length by *A*, corresponding to our interval -0.058×10^{-4} s < *t* < $+2.692\times10^{-4}$ s. It is noticed that the time scale in our figure 3 is of order 10^{-4} s, whereas the fall time of the cylinder $t_2 = 0.102$ s.

In order to evaluate left hand side of (3.4), Ohm's law will be applied to a round wire or a cylinder (see, e.g., Ramo *et al.* [11])

$$V_{ind} = iR = \frac{dQ}{dt}\frac{l}{\sigma A_{eff}}, \tag{3.6}$$

where *i* is the current and *dQ* is the amount of charge passing through a cross-section A_{eff} of a conductor in time *dt*. The electrical conductivity of the cylinder is σ. The resistance *R* is proportional to the length $l = h$ of the cylinder of radius r_0. The surface A_{eff} for frequency ω is given by

$$A_{eff} = 2\pi r_0\delta, \quad \delta = \left(\frac{2}{\mu_r\mu_0\omega\sigma}\right)^{1/2}, \tag{3.7}$$

where μ_r is the relative permeability of the conductor and μ_0 is the vacuum permeability, respectively. The quantity δ is the skin depth, i.e., the depth at which the current density has dropped to 1/e = 0.3679 of its surface value. Utilizing the values $\mu_r \approx 1$ and $\mu_0 = 4\pi\times10^{-7}$ $N.A^{-2}$ and $\sigma = 5.96\times10^7$ $S.m^{-1}$ for the copper cylinder in Woodward's experiment [1], the following values for δ can be calculated from (3.7) for the estimates of ω_1 and ω: $\delta_1 = 6.84\times10^{-4}$ m and $\delta = 1.53\times10^{-3}$ m, respectively. These small values show that the current mainly flows near the surface of the wire or cylinder.

As a consequence of the skin effect, the current $i = dQ/dt$ near the surface of the cylinder ($r \to r_0$) will be larger than for radii *r* approaching zero value ($r \to 0$). Combination of (3.4) through (3.7) then yields for the total current *dQ*/*dt*

$$\frac{dQ}{dt} = \pi r_0^2\sigma\delta\left\{\omega_1\sin\omega_1 t + \omega\sin\omega t + a\left(\cos\omega_1 t + \cos\omega t\right)\right\}e^{-at}B_{\varphi 2}(r_0). \tag{3.8}$$

Integration of *dQ* in (3.8) from time $t = t_1$ up to time $t = t_2$ then yields for the charge *Q*

$$Q = -\pi r_0^2\sigma\delta\left\{\left(\cos\omega_1 t_2 + \cos\omega t_2\right)e^{-at_2} - \left(\cos\omega_1 t_1 + \cos\omega t_1\right)e^{-at_1}\right\}B_{\varphi 2}(r_0). \tag{3.9}$$

For Woodward's copper cylinder [1] the induced charge *Q* between times t_1 and t_2 can be calculated from (3.9) by inserting the values $r_0 = 0.025$ m, $\sigma = 5.96\times10^7$ $S.m^{-1}$ for copper, $\delta = 1.53\times10^{-3}$ m, corresponding to ω, the value of $B_{\varphi 2}(r_0)$ from (2.7) (a value $\beta = +1$ will be adopted) and the estimated values of *a*, ω_1 and ω. For the time interval -0.058×10^{-4} s < *t* < 0.565×10^{-4} s one obtains a charge $Q = -1.93\times10^{-12}$ C. This result corresponds to the charge under the first subpulse (designated by *B* in Woodward's figure 3). In addition, a charge $Q = -1.95\times10^{-12}$ C can be calculated for the time interval -0.058×10^{-4} s < *t* < 2.692×10^{-4} s (this interval corresponds with the length of the

initial pulse *A* in Woodward's figure 3). The induced charges corresponding with signals *A* and *B* are both negative in his figure 3, in agreement with our calculated charges for *Q*. Finally, for the interval 2.692×10^{-4} s < *t* < 5.442×10^{-4} s calculation from (3.9) yields a small, *positive* charge $Q = +\ 1.25\times10^{-13}$ C.

The observed charges for falling cylinders of copper, steel and aluminium from Woodward [1] have been summarized in table 1. From a regression analysis the ratio of the observed absolute values of the induced charge $|Q|$ to speed $|v_z|$, $|Q|/|v_z|$, have been calculated (note that both Q and v_z have a negative sign). The high values of the correlation coefficients show the apparent proportionality between Q and v_z. The deviation from theory can be quantified by the parameter β. Its sign is positive, but in view of the large discrepancy between observations and theory this result is not significant.

Table 1. Observed values of $|Q|/|v_z|$ for the first subpulse *B* of three metal samples from Woodward [1] are compared with the corresponding predicted values from (3.9). The induced charges *Q* have been calculated for the isolator fluids pentane and benzene. For comment see text.

Cylinder of	*m* (kg)	solvent	$\lvert Q\rvert/\lvert v_z\rvert$ observed (C.m^{-1}.s)	correlation coefficient	σ (S.m^{-1})	$\lvert Q\rvert/\lvert v_z\rvert$ predicted[a] (C.m^{-1}.s)	β
copper	1.233	pentane benzene	2.04×10^{-11} 2.09×10^{-11}	0.998 0.993	5.96×10^{7} 5.96×10^{7}	1.93×10^{-12} 1.93×10^{-12}	+ 10.6 + 10.8
steel	1.081	pentane benzene	2.01×10^{-11} 2.04×10^{-11}	0.999 0.991		[b]	
aluminium	0.473	pentane benzene	1.73×10^{-11} 1.57×10^{-11}	1.000 0.998	3.5×10^{7} 3.5×10^{7}	1.48×10^{-12} 1.48×10^{-12}	+ 11.6 + 10.6

[a] Copper and aluminium are nearly non-magnetic, so that for both metals the vacuum value $\mu_r = 1$ for the relative permeability can be used. For the calculation of $|Q|/|v_z|$ for aluminium the value of *f(t)* for copper has been used. [b] For ferromagnetic steel $\mu_r > 0$. In that case this factor has to be added to the r. h. s. of (2.1). Since the values for μ_r and the conductivity σ for the used type of steel are not known, the theoretical value for $|Q|/|v_z|$ cannot be calculated for the cylinder of steel.

Although the largest charges *Q* are obtained for the massive copper and steel samples, there seems no clear correlation between sample mass *m* and charge *Q*. Note that a proportionality between $B_{\varphi 1}$ and *m* is predicted by (2.7). In addition, a proportionality is predicted between the charge *Q* of (3.9) and the conductivity σ of the sample. Comparison of charges *Q* for copper and aluminium samples shows a larger charge for copper, but no proportionality is found between *Q* and σ.

4. GRAVITOMAGNETIC FIELD OF A ROTATING CYLINDER

The stationary value of the gravitomagnetic induction field **B** from a rotating body can be calculated by combining (2.1a) and (2.4)

$$\nabla\times\mathbf{B} = -\frac{\beta\mu_0 G^{1/2}}{k^{1/2}}\rho\,\mathbf{v} \quad \text{and} \quad \nabla\cdot\mathbf{B} = 0, \tag{4.1}$$

where $\mathbf{v} = \boldsymbol{\omega}\times\mathbf{r}$ is a rotational velocity. Since $\nabla\cdot\mathbf{B} = 0$, the field **B** can be derived from a gravitomagnetic vector potential **A** ($\mathbf{B} = \nabla\times\mathbf{A}$). For a massive rotating sphere with radius r_0 and angular momentum **S** and the following expression for the vector potential **A** can be deduced from (4.1) (see, e.g., [6-8, 12])

$$\mathbf{A} = \frac{\mu_0}{4\pi}\frac{\beta G^{1/2}}{2k^{1/2}}\mathbf{S}\times\nabla\left(1/R\right) = -\frac{\mu_0}{4\pi}\frac{\beta G^{1/2}}{2k^{1/2}}\frac{\mathbf{S}\times\mathbf{R}}{R^3}. \tag{4.2}$$

Here **R** is the position vector from the centre of the sphere to the field point *F*, where the vector potential **A** is measured (*R* is the scalar value of **R**; $R \geq r_0$). The expression for **A** in (4.2) can be rewritten in terms of the gravitomagnetic dipole moment **M**(gm) defined by

$$\mathbf{M}(\mathrm{gm}) = -\frac{\mu_0}{4\pi}\frac{\beta G^{1/2}}{2k^{1/2}}\mathbf{S}. \tag{4.3}$$

Introduction of (4.3) into (4.2), followed by evaluation of $\mathbf{B} = \nabla \times \mathbf{A}$, yields for the gravitomagnetic induction field **B**

$$\mathbf{B} = \nabla\left(\mathbf{M}\cdot\nabla\frac{1}{R}\right) = \left(\frac{3\mathbf{M}\cdot\mathbf{R}}{R^5}\mathbf{R} - \frac{\mathbf{M}}{R^3}\right). \tag{4.4}$$

For a cylinder with homogeneous mass density ρ, radius r_0 and total mass *m* the angular momentum **S** is given by

$$\mathbf{S} = I\boldsymbol{\omega}, \quad \text{and} \quad S = I\omega = \tfrac{1}{2}\, m r_0^2 \omega, \tag{4.5}$$

where $\boldsymbol{\omega}$ is the angular momentum vector ($\omega = 2\pi v$ is the angular velocity of the cylinder and *v* is its rotational frequency), *I* is the moment of inertia of the cylinder. Expressions (4.2) through (4.4) also apply to a cylinder, when *R* is much larger than the radius r_0 and height *h* of the cylinder. The gravitomagnetic field in the equatorial plane of the cylinder is then given by

$$\mathbf{B}_{\mathrm{eq}}(\mathrm{gm}) = -\frac{\mathbf{M}(\mathrm{gm})}{R^3} = \frac{\mu_0}{4\pi}\frac{\beta G^{1/2} m r_0^2 \boldsymbol{\omega}}{4k^{1/2}R^3}. \tag{4.6}$$

The right hand side of (4.6) has been calculated by utilizing (4.3) through (4.5).

In table 2 data from Surdin [3, 4] are summarized for rotating cylinders of bronze and of a tungsten alloy, respectively. Radius r_0 and height *h* are the same for both metal cylinders (r_0 = 0.05 m and height *h* = 0.15 m). Observed, absolute values of the equatorial magnetic induction field B_{eq}(em) from [4] are given in table 2. It appeared (see ref. [3, p. 505]) that the magnetic induction fields from the cylinder of bronze and tungsten reversed on a time scale of 3.5×10^{-5} s and 4.5×10^{-5} s, respectively. Because of these rapid reversals, measurements of the equatorial field B_{eq}(em) became more accurate (see eq. (3.1)). The values of B_{eq}(em) are compared with the corresponding gravitomagnetic fields B_{eq}(gm) from (4.6) for $R = r_0$. It appears that the values of β deduced from observations have nearly unity value. So, observed and predicted values for the fields B_{eq}(em) are in fair

Table 2. Data for two non-magnetic ($\mu_r \approx 1$) rotating samples are given. Observed absolute values of the equatorial field B_{eq}(em) from Surdin [3, 4] are compared with the corresponding predicted gravitomagnetic fields B_{eq}(gm) from (4.6) for $R = r_0$. For comment see text.

Cylinder of	m[a] (kg)	ω[b, c] (s^{-1})	r_0[a] (m)	h[a] (m)	B_{eq}(em)[c] observed (T)	B_{eq}(gm) predicted (T)	β
bronze	10.36	2.827×10^{3}	0.05	0.15	1.8×10^{-12}	1.26×10^{-12}	1.4
tungsten alloy	20.73	2.733×10^{3}	0.05	0.15	1.9×10^{-12}	2.44×10^{-12}	0.78

[a] Ref. [3], from p. 495. [b] Ref. [3], p. 504. [c] Ref. [4], p 141, p 142.

agreement for $\beta = +1$. These results may reflect the approximate validity of the so-called Wilson-Blackett formula, embodied in relation (4.3).

In order to explain the observed fields B_{eq}(em), Surdin [3, 4] assumed the existence of a universal fluctuating electromagnetic field. This field may induce electric dipoles in an otherwise electrically neutral rotating body. For the case of a rotating sphere of radius r_0 he deduced the following mean square amplitude of the electromagnetic field B_c(em) in the centre of the sphere

$$\langle B_c^2(\text{em})\rangle = \left(\frac{\mu_0}{4\pi}\right)^2 \frac{Gm^2\omega^2}{8kr_0^2}. \tag{4.7}$$

This result can be compared with the corresponding gravitomagnetic field B_c(gm) in the centre of the sphere deduced by Biemond [13, p. 10]

$$\mathbf{B}_c(\text{gm}) = -\frac{\mu_0}{4\pi}\frac{\beta G^{1/2} m\boldsymbol{\omega}}{k^{1/2} r_0} \quad \rightarrow \quad B_c^2(\text{gm}) = \left(\frac{\mu_0}{4\pi}\right)^2 \frac{\beta^2 Gm^2\omega^2}{kr_0^2}. \tag{4.8}$$

Equalizing the fields B_c(em) of (4.7) and B_c(gm) of (4.8), would result into a value for the parameter β of $\beta = \pm 8^{-1/2} = \pm 0.345$. It is noticed, that for a sphere the gravitomagnetic field in the equatorial plane at distance $R = r_0$, corresponding to B_c(gm) in (4.8), can be calculated to be (see ref. [13, p. 11])

$$\mathbf{B}_{eq}(\text{gm}) = \frac{\mu_0}{4\pi}\frac{\beta G^{1/2} m\boldsymbol{\omega}}{5k^{1/2} r_0}. \tag{4.9}$$

So, for a sphere $\mathbf{B}_{eq}$(gm) = – 1/5 $\mathbf{B}_c$(gm). Note that the value of $\mathbf{B}_{eq}$(gm) in (4.9) is a factor 4/5 smaller than that of $\mathbf{B}_{eq}$(gm) in (4.6) for $R = r_0$. This difference is caused by a difference in the angular momentum **S**: for a sphere this quantity is a factor 4/5 smaller than for a cylinder.

Equations (4.1)–(4.5) can also be applied to spherical stars consisting of electrically neutral matter. The identification of the "magnetic-type" gravitational field with a magnetic field then again leads to the Wilson-Blackett formula (4.3). Available observations and theoretical considerations with respect to the relation (4.3), and alternative explanations of the origin of the magnetic field of celestial bodies have been reviewed by Biemond [7]. The magnetic field of pulsars has separately been discussed in ref. [14].

5. DISCUSSION OF THE RESULTS

Induced charges in metal samples falling onto an impact plate were observed by Woodward [1]. He carefully checked conventional charge-generating mechanisms as an explanation for the observed charges, but found none. Especially, he examined a possible piezoelectric effect by bolting a 1.370 kg brass cylinder to the piston. This additional mass should increase the induced charges. As can be seen from his figure 5 and table III, however, the induced charges in the first subpulses appeared to be virtually unaffected by this addition of mass. Therefore, he concluded that piezoelectric effects must be rejected as source of the observed signals.

Woodward tried to explain the observed signals in terms of relation (1.1). He indeed found a linear dependence between the induced charges Q and the impact velocity v_z, but he found no quantitative correlation between mass m of the cylinder and induced charges Q. To our knowledge, no alternative explanations for the observed charges have

not been given since 1980.

The final result of our gravitomagnetic approach, embodied in (3.9), predicts values for Q an order of magnitude smaller than observed. Comparison of charges Q for copper and aluminium samples shows a larger charge for copper with the highest value of σ, but no proportionality is found between Q and σ. It is noticed that the observations of induced charges Q provide no direct evidence for the existence of generated gravitomagnetic fields like $B_{\varphi 2}$ in (2.7). At present, the explanation for the generation of the observed charges has not yet been confirmed quantitatively. However, the applied special interpretation of the gravitomagnetic theory may be helpful in explaining other cases where air/water/dust is rising or falling and charge generation is observed, e.g., hurricanes, tornados, thunderstorms, dust devils and waterfalls. All these phenomena have in common that the predicted gravitomagnetic fields, corresponding to $B_{\varphi 2}$ in (2.7), are weak.

The generation of a gravitomagnetic field by a rotating metal sample has been considered in section 4. Surdin [3, 4] observed magnetic induction fields B_{eq}(em) at the equator of rotating cylinders of bronze and tungsten, respectively. In table 2 observed, absolute values of the equatorial field B_{eq}(em) from Surdin [4] are compared with the corresponding predicted gravitomagnetic fields B_{eq}(gm) from (4.6). Within experimental error the found agreement of both fields is an indication of the validity of our gravitomagnetic approach. No explanation for the field reversals, however, has been given.

Summing up, more experimental evidence and theory will be necessary to elucidate the origin of the induced charges of falling metal cylinders observed by Woodward [1]. The magnetic induction fields near rotating cylinders observed by Surdin [3, 4] can be explained by our approach. More study of the nature of the gravitomagnetic induction fields like given in (2.7) and (4.6) is needed, however, as has been discussed previously [12].

REFERENCES

[1] Woodward, J. F., "An experimental reexamination of Faradayan electrogravitational induction." *Gen. Rel. Grav.* **12**, 1055-1069 (1980).

[2] Woodward, J. F., "Electrogravitational induction and rotation." *Found. Phys.* **12**, 467-478 (1982).

[3] Surdin, M. "Magnetic field of rotating bodies." *J. Franklin Inst.* **303**, 493-510 (1977).

[4] Surdin, M. "Le champ magnétique des corps tournants." *Ann. Fond. L. de Broglie* **5**, 127-145 (1980).

[5] Luchak, G., "A fundamental theory of the magnetism of massive rotating bodies." *Can. J. Phys.* **29**, 470-479 (1951).

[6] Biemond, J., *Gravi-magnetism*, 1st ed. (1984). Postal address: Sansovinostraat 28, 5624 JX Eindhoven, The Netherlands. E-mail: j.biemond@gravito.nl Website: http://www.gravito.nl

[7] Biemond, J., *Gravito-magnetism*, 2nd ed. (1999). See also ref. [6].

[8] Biemond, J., "Which gravitomagnetic precession rate will be measured by Gravity Probe B?", arXiv:physics/0411129v1 [physics.gen-ph], 13 Nov 2004.

[9] Blackett, P. M. S., "The magnetic field of massive rotating bodies." *Nature* **159**, 658-666 (1947).

[10] Wilson, H. A., "An experiment on the origin of the Earth's magnetic field." *Proc. R. Soc. A* **104**, 451-455 (1923).

[11] Ramo, S., Whinnery, J. R. and Van Duzer, T., *Fields and waves in communication electronics*, 3rd ed. (1994), John Wiley & Sons, p. 180-186.

[12] Biemond, J., "The gravitomagnetic field of a sphere, Gravity Probe B and the LAGEOS satellites", arXiv:0802.3346v2 [physics.gen-ph], 14 Jan 2012.

[13] Biemond, J., "The gravitomagnetic vector potential and the gravitomagnetic field of a rotating sphere." viXra:astrophysics/1205.0064v1, 15 May 2012.

[14] Biemond, J., "The origin of the magnetic field of pulsars and the gravitomagnetic theory." In: *Trends in pulsar research* (Ed. Lowry, J. A.), Nova Science Publishers, New York, Chapter 2 (2007) (updated and revised version of arXiv:astro-ph/0401468v1, 22 Jan 2004).